Stability Of A Flat Strip Of Fabric Loaded With Compression Forces

Piotr Szablewski

Department of Mechanical Engineering, Informatics and Chemistry of Polymer Materials,
Lodz University of Technology, Lodz, Poland

Abstract: *This paper deals with a method for examining the state of equilibrium of a heavy elastica. Such object is used e.g. for modeling a flat textile structure loaded with its dead weight and axial force. The elastica represents a longitudinal section of a fabric. It was assumed that the elastica rests on a flat, immovable base. Only those forms of deformed elastica were considered where its two ends were supported by pivot bearings, and the tangent at those points lay on the immovable supporting plane. In the analysis, shape of the deflection curve was determined for a given axial force, and it was examined whether a given position is stable or unstable. The analysis was made on the basis of the energetic method, by examining potential energy of the system. The investigations can be used for simulation of fabric buckling, folding and for another applications from the field of textile mechanics.*
Keywords*: stability; elastica; deflection curve; states of equilibrium; bending theory.*

I. Introduction

Stability analysis of various mechanical structures is one of the most frequently undertaken research topics. This issue is not simple and often requires complex analysis. Similarly, considering large deflections of a structure (e.g. shells, plates or beams) leads to complicated solutions. In the problems of textile mechanics, large deflections are very often taken into account, as well as stability problems. Due to the fact that the mechanics of textiles is a relatively young field of science, many problems occurring in it are solved on the basis of classical mechanics, the theory of elasticity, etc. In addition, classical theory of "elastica" is often used to analyze linear and flat textile structures.

Greenhill [1] first correctly found the stability criteria for a standing uniform heavy cantilever. Various aspects of the uniform heavy elastica cantilever have been reported previously, e.g. [2-8]. The stability for the vertical pointy heavy cantilever, i.e. the tip tapered into a sharp point, was solved by Dinnik [9] in terms of Bessel functions. The stability of a beam under a concentrated force, which is clamped at one end while sliding over a point support at the other, has been studied in [10]. The slip-through of a beam under self-weight resting on two point supports has been examined in [11].

Thick plate analysis involves research areas such as plate vibration, bending and buckling [12]. Under the influence of in-plane compressive loads, the plate material gradually becomes unstable at the critical value of the loads. This phenomenon is called buckling [13,14]. Based on the stress-strain relationship, plate buckling problem is classified as elastic and inelastic (plastic) buckling. When the critical buckling load is smaller than the elastic limit of the plate material, it is considered as the elastic buckling problem otherwise the problem is called inelastic buckling [15]. The classical methods also called the equilibrium (Euler) methods are analytical methods that seek to obtain closed form solutions for solving the governing partial differential equilibrium equations of the plate buckling problem within the plate domain, subject to the boundary conditions of loading and the restraints of the plate edges [16]. To obtain approximate solutions to the plate problem, numerical methods are used. These methods include the weighted residual methods, finite difference methods, finite element methods, and finite strip methods [17]. To overcome the rigorous routine inherent in classical and numerical methods, variational method can be applied. The energy methods such as Ritz variational method, Kantorovich variational method, Rayleigh-Ritz method, and Galerkin method; with respect to the displacement function minimizes the total potential energy functional to derive the characteristic buckling equation from which the buckling loads are obtained.

Series of theories has been developed and applied to analyze the buckling behavior of plates. One of these theories is the classical plate theory (CPT) [18], which is mostly employed in the analysis of thin plates, underestimates deflections, and over-estimates buckling loads and natural frequencies in thick plates.

Mindlin [19] proposed the shear deformation plate theories to overcome the limitations of CPT [18,20]. These theories are also called the Refined Plate Theories (RPT) which consists of first-order shear deformation theory (FSDT) and higher-order shear deformation theories (HSDT) [21-23]. Authors in [24], employed refined

trigonometric shear deformation plate theory to analyze the buckling behavior of a simply supported plate under both biaxial and uniaxial compression using the virtual work principle. The result obtained from the study showed excellent agreement when compared with other refined theories. The polynomial shape functions were used by the authors in [25,26] analyzed the buckling behavior of the same thick rectangular plate that is simply supported under uniaxial compressive loading. To derive the governing equations of the plate, the authors applied polynomial shape theory. The equation for formulating the non-dimensional critical buckling load parameters of the plates was obtained by solving the direct governing equation with satisfied plate boundary conditions.

To analyze the buckling behavior of clamping plate, the authors in [27] adopted work principle approach. The buckling coefficients of the plate were obtained and a numerical model was developed using the polynomial displacement function. The authors did not take a thick plate into consideration as their assumption is limited to the classical plate theory which is not reliable for thick plate analysis. Their study did not apply trigonometric functions and SSFS plate was not considered.

In [28,29] the authors applied both trigonometric and polynomial displacement function to determine the critical buckling load of clamped thick rectangular plate using the analytical three-dimensional plate theory that is formulated and derived from the variational energy method, but could not apply it to a rectangular plate structure that is freely supported at the third edge and other three edges simply supported.

This paper deals with a method for examining the state of equilibrium of a heavy elastica. The elastica represents a longitudinal section of a fabric. The analysis of stability was made on the basis of the energetic method, by examining potential energy of the system. The investigations can be used for simulation of fabric buckling, folding and for another applications from the field of textile mechanics.

II.   Material And Methods

In this paper, it is assumed that during the run of bending effect the flat strip of the fabric will be represented as its longitudinal section. The mathematical model will be described as a flat deflection curve, i.e. heavy elastica as shown in Figure 1. It is assumed that the particular longitudinal sections do not act on each other by internal forces (plane stress). Furthermore, the constancy of properties along the whole width of the bending strip is assumed.
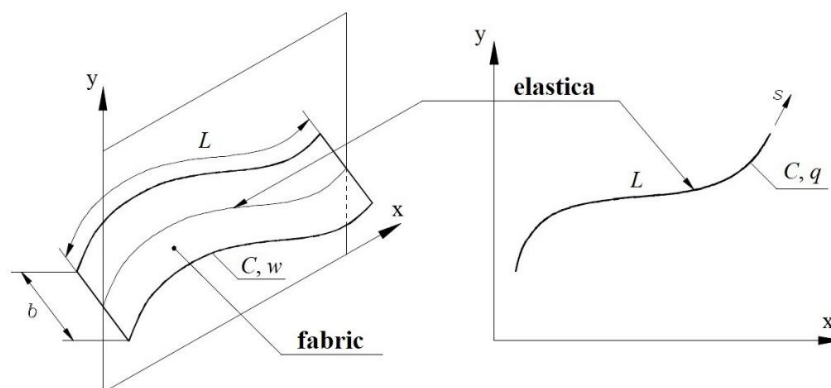
Fig. 1 The model of fabric approximated by elastica

Therefore, instead of studying the fabric strip of length L, width b, bending stiffness C and weight per unit area w, the numerical analysis will be concerned with deflections of heavy elastica of a given length L, bending stiffness C and appropriate weight per unit length q. Bending stiffness C is equivalent to the product of modulus of elasticity times the moment of inertia ($C = E \cdot I$).

Assumptions of Model and Initial Equations

Let us consider a heavy elastica resting on a fixed, immovable base Figure 2. Under the influence of compressive forces, a fold is formed, which remains there due to friction forces.

Depending on the magnitude of the friction force, this fold will either remain or disappear after the compressive forces are removed. In order to enable a thorough examination of stability of the object, a substitute model was assumed which is limited to deformed shape of elastica, i.e. to the fold.
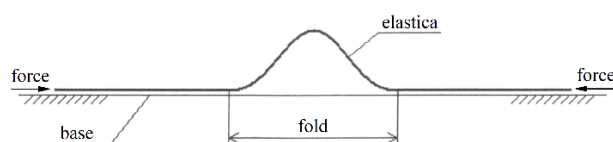
Fig. 2 The model of fabric approximated by elastica

Let heavy elastica be loaded with the axial force *P* and continuous load *q* (weight per unit length) in the coordinate system as in Figure 3. The elastica rests on a flat, fixed surface and is pinned at points A and B. At these points there is a swivel joint. The elastica is non-extensible so it cannot change its length *L* under the influence of loads acting on it. The established theory of bending is expressed in the following formula

$$M = EI\frac{1}{\rho} \tag{1}$$

where *ρ* is the radius of curvature, *EI* the bending stiffness and *M* the bending moment. There are no simplifications in terms of curvature 1/*ρ*, as in the case of the theory of bending beams, because large deformations occur.
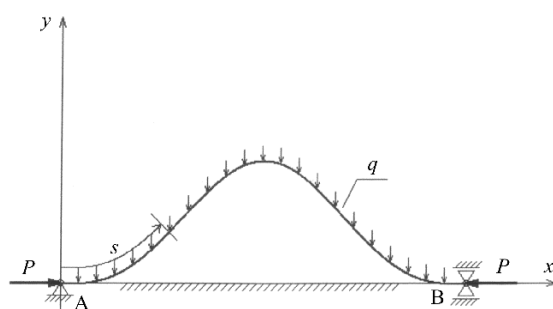
Fig. 3 The load scheme of the elastica in the coordinate system

In this case, the existence of a rigid surface constrains the *y* coordinate. This one must be greater or equal to zero for each value of the arc coordinate s, which is measured along the deflection curve. The boundary conditions for this load scheme are as follows.

$$y = 0\big|_{s=0} \, , \, y = 0\big|_{s=L}$$
$$M = 0\big|_{s=0} \, , \, M = 0\big|_{s=L} \tag{2}$$

Zero moment *M* at the points of support A and B results from the fact that apart from the fold, the elastica rests flat on the surface and its curvature 1/*ρ* is equal to zero. From that fact it also results that the tangent at the points of support must be horizontal. Thus, we get additional boundary conditions, namely

$$\frac{dy}{ds} = 0\bigg|_{s=0} \, , \, \frac{dy}{ds} = 0\bigg|_{s=L} \tag{3}$$

Let us consider the infinitesimal section of elastica presented in Figure 4.
As it has been already mentioned, the elastica is non-extensible $dx^2 + dy^2 = ds^2$. Therefore we have the following geometrical condition

$$dy/ds < 1 \tag{4}$$
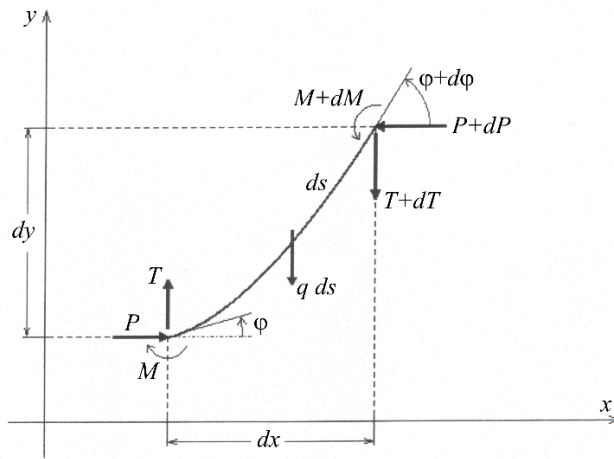
Fig. 4 The infinitesimal section of elastica

Now let's write the elementary equations of equilibrium according to Figure 4.

$$\begin{aligned} -dP &= 0 \\ -dT - qds &= 0 \\ dM - Tdx + Pdy &= 0 \end{aligned} \qquad (5)$$

Basing on the above equations of equilibrium we get the principle of virtual work on the virtual displacements δx, δy, $\delta\varphi$. To do this, we multiply the Equation 5 by appropriate virtual displacements. Then, by adding and integrating within the limits from 0 to L we obtain

$$-dP\delta x - dT\delta y - qds\delta y + dM\,\delta\varphi - Tdx\delta\varphi + Pdy\delta\varphi = 0 \qquad (6)$$

$$-\int_0^L \frac{dP}{ds}\delta x\,ds - \int_0^L \frac{dT}{ds}\delta y\,ds - \int_0^L T\frac{dx}{ds}\delta\varphi\,ds + \int_0^L P\frac{dy}{ds}\delta\varphi\,ds - \int_0^L q\delta y\,ds + \int_0^L \frac{dM}{ds}\delta\varphi\,ds = 0 \qquad (7)$$

After integrating by parts we can write

$$\begin{aligned} &-P\delta x\Big|_0^L + \int_0^L P\delta\left(\frac{dx}{ds}\right)ds - T\delta y\Big|_0^L + \int_0^L T\delta\left(\frac{dy}{ds}\right)ds - \int_0^L T\frac{dx}{ds}\delta\varphi\,ds + \\ &+ \int_0^L P\frac{dy}{ds}\delta\varphi\,ds - \int_0^L q\delta y\,ds + M\delta\varphi\Big|_0^L - \int_0^L M\delta\left(\frac{d\varphi}{ds}\right)ds = 0 \end{aligned} \qquad (8)$$

Considering that $dx/ds = \cos\varphi$, $dy/ds = \sin\varphi$ and $d\varphi/ds = 1/\rho$ and taking the boundary conditions and the Equation 1, the Equation 8 after reduction takes the form of

$$\int_0^l q\delta y\,ds + P\delta x_B + \int_0^l \frac{1}{2}EI\delta\left(\frac{d\varphi}{ds}\right)^2 ds = 0 \qquad (9)$$

Therefore

$$\delta\left[q\int_0^l y\,ds + Px_B + \frac{1}{2}EI\int_0^l \left(\frac{d\varphi}{ds}\right)^2 ds\right] = 0 \qquad (10)$$

The obtained Equation 9 represents the principle of virtual work, which provides that in the state of equilibrium the sum of work of all actual forces (both external and internal) acting on the system, for any virtual displacements, is equal to zero. The functional occurring in the square bracket in Equation 10 is total potential energy of the system (potential of external and internal forces).

$$J[y] = q\int_0^l y\,ds + Px_B + \frac{1}{2}EI\int_0^l \left(\frac{d\varphi}{ds}\right)^2 ds \tag{11}$$

The Equation 10 can be thus written in the form of

$$\delta J[y] = 0 \tag{12}$$

This is the necessary condition for existence of extremum of the functional $J[y]$. If equilibrium is stable then the potential energy reaches a minimum at equilibrium state. In the case of maximum potential energy, we deal however with the unstable state of equilibrium (labile equilibrium) [30].

Deflection Curve

As it is already known the deflection curve of the elastica in the state of equilibrium should present the extremum of functional $J[y]$ (Equation 11), respectively minimum for stable equilibrium, and maximum for labile one. In order to determine the extremum of functional, let's take for consideration the equation of the deflection curve, which fulfils given boundary conditions. Let the deflection curve be described by the Equation 13.

$$y(s) = A\sin\left(\frac{\pi s}{L}\right) + B\sin\left(\frac{3\pi s}{L}\right) \tag{13}$$

where coefficients A and B are unknown at this moment.
It can be easily noticed that the function $y(s)$ (Equation 13) fulfils the boundary conditions from Equation 2. From the additional boundary conditions (Equation 3) we get the relationship between the coefficients A and B in the form of $B = -\frac{1}{3}A$. After transformations, the deflection curve is defined by the equation

$$y = \frac{4}{3}A\sin^3\left(\frac{\pi s}{L}\right) \tag{14}$$

The range of admissible values of A parameter will be presented in the next point.

Admissible Values for the Shape Parameter

We have the deflection curve defined by the Equation 14. The shape parameter A occurring in the equation will be hereafter presented in the dimensionless form $a = A/L$, related to the length L. This parameter cannot take full range of values. Below there is a precise definition of the interval of admissible values of a. According to the assumptions and the introduced coordinate system $y \geq 0$. Thus

$$\frac{4}{3}A\sin^3\left(\frac{\pi s}{L}\right) \geq 0 \tag{15}$$

Since we discuss only the interval from $s = 0$ to $s = L$, then from the properties of the function y it follows that $A \geq 0$ and hence

$$a \geq 0 \tag{16}$$

Apart from that, in the model assumptions the Equation 4 was given (non-extensible elastica). Applying it now, and substituting $\xi = \pi s/L$ in the interval $0 \leq \xi \leq \pi$ we get

$$4a\pi \sin^2(\xi)\cos(\xi) < 1 \tag{17}$$

To find the value a first we determine the maximum value of the function f within the interval $0 \leq \xi \leq \pi$

$$f = \sin^2(\xi)\cos(\xi) \tag{18}$$

because in order to satisfy Equation 17, it is enough to substitute the maximum value of the *f* function from Equation 18. By examining the function *f*, it can be proved that in the given interval it has only one maximum amounting to: $f_{mx} = 2/(3\sqrt{3})$.

From Equation 17 we get: $8a\pi/(3\sqrt{3}) < 1$. Therefore

$$a < 3\sqrt{3}/(8\pi) \cong 0.2067 \tag{19}$$

So, we have obtained the following interval of admissible values of the shape parameter

$$0 \leq a < a_{gr} = 3\sqrt{3}/(8\pi) \tag{20}$$

Potential Energy of the System

Let us consider for the functional from Equation 11 the deflection function described by the Equation 14. After substituting this function in the Equation 11 *J*[*y*] becomes a function of a single variable *A*: $J[y] = V(A)$.

To find the value of coefficient *A* the Ritz method be applied. The method uses the necessary condition of existence of extreme of *V*(*A*).

$$dV/dA = 0 \tag{21}$$

The Equation 11 must be first transformed and integrals calculated. For the first component we have

$$q\int_0^L y\,ds = q\int_0^L \frac{4}{3}A\sin^3\left(\frac{\pi s}{L}\right)ds = \frac{16qL}{9\pi}A \tag{22}$$

In the second component of Equation 11 there is the x_B value which is the *x* coordinate of the movable end of elastica:

$$x_B = \int_0^L \sqrt{1 - \left(\frac{dy}{ds}\right)^2}\,ds \cdot$$

Since this integral cannot be calculated exactly, the approximate square root formula must be used.

$$x_B \cong \int_0^L \left[1 - \frac{1}{2}\left(\frac{dy}{ds}\right)^2\right]ds = \int_0^L ds - \frac{1}{2}\int_0^L \left(\frac{dy}{ds}\right)^2,$$

$$x_B \cong l - \frac{1}{2}\int_0^L \left[\frac{4A\pi}{L}\sin^2\left(\frac{\pi s}{L}\right)\cos\left(\frac{\pi s}{L}\right)\right]^2 ds$$

After transformation, we obtain

$$x_B = L - \frac{\pi^2 A^2}{2L} \tag{23}$$

Therefore

$$P\,x_B = PL - \frac{P\pi^2 A^2}{2L} \tag{24}$$

Before calculation of the third component, it is necessary to represent the curvature $d\varphi/ds$ in a somewhat different form. It is known that

$$\frac{d\varphi}{ds} = \frac{d^2 y/ds^2}{\sqrt{1 - (dy/ds)^2}} \tag{25}$$

Now the integral has to be calculated.

$$\int\limits_0^L \left(\frac{d\varphi}{ds}\right)^2 ds = \int\limits_0^L \left(\frac{d^2 y/ds^2}{\sqrt{1-(dy/ds)^2}}\right)^2 ds = \int\limits_0^L \frac{(d^2 y/ds^2)^2}{1-(dy/ds)^2} ds$$

As it is impossible to represent the result of the above integration in the form of elementary functions, an approximate solution is to be applied. To do this, the numerator and denominator of the integral are multiplied by $1+(dy/ds)^2$.

$$\int\limits_0^L \frac{(d^2 y/ds^2)^2 [1+(dy/ds)^2]}{1-(dy/ds)^4} ds \tag{26}$$

Since, as it was shown at the beginning: $dy/ds < 1$, then $(dy/ds)^4$ is much less than 1. It can be thus assumed that $1-(dy/ds)^4 \cong 1$, and thus it follows

$$\int\limits_0^L \left(\frac{d\varphi}{ds}\right)^2 ds \cong \int\limits_0^L (d^2 y/ds^2)^2 \left[1+(dy/ds)^2\right] ds \tag{27}$$

A better approximation can be obtained by subsequent multiplication of the numerator and denominator of the Equation 26 by $1+(dy/ds)^4$ and so on. Applying in Equation 27 the formulas for the first and second derivatives of the y function, we obtain after integration

$$\frac{1}{2} EI \int\limits_0^L \left(\frac{d\varphi}{ds}\right)^2 ds = \frac{EI\pi^4}{8L^5} \left(20L^2 A^2 + 13\pi^2 A^4\right) \tag{28}$$

The formula for the total potential energy of the system finally takes the form

$$V(A) = \frac{16qL}{9\pi} A + PL - \frac{P\pi^2}{2L} A^2 + \frac{5EI\pi^4}{2L^3} A^2 + \frac{13EI\pi^6}{8L^5} A^4 \tag{29}$$

The potential energy is so the function of the single variable A which can be called a variable parameter of shape, and two constants connected with the external load, namely P and q.

III. Results and Discussion

Analysis of States of Equilibrium

To begin analysis of the states of equilibrium, the above-mentioned condition (Equation 21) is to be applied, on basis of which the value of the shape parameter A can be determined. It is the parameter on that the kind of equilibrium depends with a given load defined by P and q.

$$\frac{dV}{dA} = \frac{16qL}{9\pi} - \frac{P\pi^2}{L} A + \frac{5EI\pi^4}{L^3} A + \frac{13EI\pi^6}{2L^5} A^3 = 0 \tag{30}$$

From the Equation 30 the following relationship between the force P and parameter A is calculated.

$$P = \frac{16qL^2}{9\pi^3} \frac{1}{A} + \frac{5EI\pi^2}{L^2} + \frac{13EI\pi^4}{2L^4} A^2 \tag{31}$$

Let us represent the energy V, force P and continuous load q in the dimensionless form, relating them to Euler critical force $P_{cr} = \pi^2 EI / L^2$.

$$a = \frac{A}{L} \;,\; p = \frac{P}{P_{cr}} \;,\; w = \frac{qL}{P_{cr}} \;,\; v = \frac{V}{P_{cr} L} \tag{32}$$

Thus, we get

$$v = p - \frac{\pi^2}{2} pa^2 + \frac{5\pi^2}{2} a^2 + \frac{13\pi^4}{8} a^4 + \frac{16w}{9\pi} a \qquad (33)$$

$$p = 5 + \frac{13\pi^2}{2} a^2 + \frac{16w}{9\pi^3} \frac{1}{a} \qquad (34)$$

Since the Equation 34 was obtained by use of the Equation 21 (necessary condition for extremum), thus points lying on the *p* curves correspond to extreme of the function of potential energy. The minimum and maximum of energy must still be defined. Therefore the second derivative of the potential energy must be zero

$$\frac{d^2V}{dA^2} = -\frac{P\pi^2}{l} + \frac{5EI\pi^4}{l^3} + \frac{39EI\pi^6}{2l^5} A^2 = 0$$

Using it, we get

$$g = \frac{P}{P_{cr}} = \frac{39\pi^2}{2} a^2 + 5 \qquad (35)$$

The curve *g* described by the Equation 35 is a diagram of the compressing force *p* represented as function of the parameter *a*, but corresponding only to the points for which the second derivative d^2v/da^2 is equal to zero.

Figure 5 presents dependence of the force *p* on the dimensionless parameter *a* for several values *w*. The curve *g* is also plotted in this figure. This is a boundary curve. On its left side on each of the *p*-curves there are points for which $d^2v/da^2 > 0$ (the minimum of potential energy *v* - stable equilibrium). It should be pointed out that the curve *g* crosses the functions *p* in their minimal points. The boundary value of the shape parameter a_{gr} is also marked on the graph.
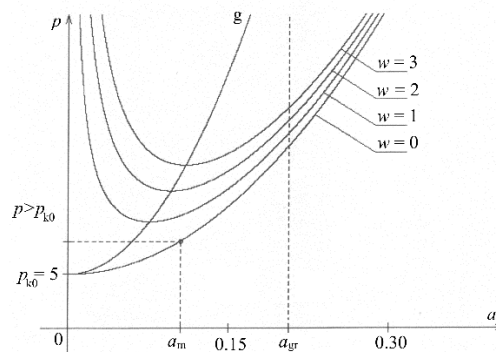
Fig. 5 Graph of the compressive force *p* as a function of the parameter *a*

Discussion of the Obtained Results

Now let us discuss in more detail the states of equilibrium for two possible cases of continuous load *w* (*w* = 0 and *w* > 0). It should be remembered that everything is considered with the condition *a* > 0.

Case I (*w* = 0).

Here are considered Figure 4 and the formulas of potential energy *v* and its derivatives. Substituting *w* = 0 in the Equation 33 we have

$$v = p - \frac{\pi^2}{2} pa^2 + \frac{5\pi^2}{2} a^2 + \frac{13\pi^4}{8} a^4$$

$$\frac{dv}{da} = -\pi^2 pa + 5\pi^2 a + \frac{13\pi^4}{2}a^3$$

$$\frac{d^2v}{da^2} = -\pi^2 p + 5\pi^2 + \frac{39\pi^4}{2}a^2$$

It should be pointed out that that minimal value of the force p amounts to $p_{k0}=5$ and it occurs with $a=0$.

- If $p < p_{k0}$, then the function v has the only extremum for $a = 0$ and it is minimum ($dv/da = 0$, $d^2v/da^2 > 0$ for $a = 0$).
- If $p = p_{k0}$, then the function v also has its minimum for $a = 0$, but it is more flat in this point.
- If $p > p_{k0}$, then the derivative dv/da when $a>0$ has already two zero points: one for $a = 0$, the other for $a = a_m$ defined by the equation

$$a_m = (1/\pi)\sqrt{2(p-5)/13} \tag{36}$$

It can be checked that for $a = 0$ the derivative $d^2v/da^2 < 0$, so in this point there is the maximum of potential energy v. But, for $a = a_m$ the derivative $d^2v/da^2 > 0$, so there is the minimum of potential energy v.

To conclude, for $p \leq p_{k0}$ there exists only the rectilinear form of equilibrium, that is the stable position is only for $a=0$. However if $p > p_{k0}$, there are two positions of equilibrium. First one, for $a = 0$ is unstable, whereas the other, for a_m defined by the Equation 36 is the position of a stable equilibrium.

Case II ($w > 0$)
As above, the formulas for potential energy v and its derivatives are considered.

$$v = p - \frac{\pi^2}{2}pa^2 + \frac{5\pi^2}{2}a^2 + \frac{13\pi^4}{8}a^4 + \frac{16w}{9\pi}a$$

$$\frac{dv}{da} = -\pi^2 pa + 5\pi^2 a + \frac{13\pi^4}{2}a^3 + \frac{16w}{9\pi}$$

$$\frac{d^2v}{da^2} = -\pi^2 p + 5\pi^2 + \frac{39\pi^4}{2}a^2$$

Basing on Figure 5 it can be seen that the minimal value of the force p, which for further consideration will be marked as p_k, is greater than it was in the previous situation for $w = 0$ ($p_k > p_{k0} = 5$). It can be also seen that the minimum occurs with $a > 0$. Let this point be designated as a_k like in Figure 6. To determine the values p_k and a_k the minimum of the function p given by the Equation 34 must be found. After appropriate transformation, we obtain

$$p_k = 5 + \sqrt[3]{416w^2/(3\pi^4)} \tag{37}$$

$$a_k = \sqrt[3]{16w/(117\pi^5)} \tag{38}$$
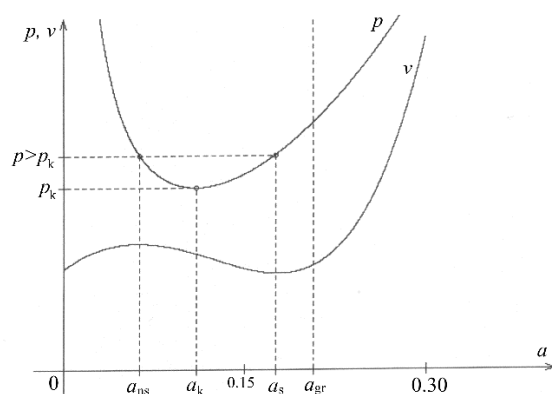
Fig. 6 An example of a graph of the compressing force p for $w = 3$ and potential energy v for $w = 3$ and $p = 8$

- If $p < p_k$, then the function v in the interval for $a \geq 0$ has no extremum. In the point $a = 0$ and for each $a > 0$ the derivative $dv/da > 0$, so the function v is increasing while the value a increases. From the function analysis it follows that for $a = 0$ the potential energy accepts the least value in the present interval.

- If $p = p_k$, then for $0 < a < a_k$ the derivative $dv/da > 0$, so the function v is increasing. In the point $a = a_k$ derivatives of the function v up to the second degree inclusive with respect to a, are equal to zero, while $d^3v/da^3 > 0$ which means that in this point there is the point of inflexion. For $a > a_k$ it again $dv/da > 0$, so in this interval the function v is increasing again.

- The situation of $p > p_k$ is illustrated as example in Figure 6 together with the graph of the force p for $w = 3$ and of the potential energy v in case when $w = 3$ and $p = 8 > p_k$ (for our example $p_k = 7.3399$ and $a_k = 0.1103$). In point $a = 0$ the derivative $dv/da > 0$. Based on Figure 6 it can be clearly seen that while increasing the value a from point $a = 0$ the function v is increasing up to the local maximum which is attained at $a = a_{ns}$. Then the function is decreasing till the local minimum occurring at $a = a_s$, and increases again.

To conclude, if $p < p_k$, then there is only a rectilinear form of stable equilibrium (state of stability for $a = 0$).

If $p = p_k$, then the stable equilibrium occurs also for the point $a = 0$ while at the point $a = a_k$ there is the critical state in which the neutral equilibrium occurs (the point of inflexion on the graph of energy v).

For $p > p_k$ there are three forms of equilibrium.

1. Rectilinear form for $a = 0$ corresponds with the state of stable equilibrium.

2. Curvilinear form corresponding to the left part of the curve (for $a = a_{ns}$) is unstable (local maximum of energy v).

3. Curvilinear form corresponding to the right part of the curve (for $a = a_s$) is stable (local minimum of energy v).

Let us now calculate the points a_s and a_{ns}. Considering that $a \geq 0$ let multiply both sides of the Equation 34 by a. We obtain then

$$\frac{13\pi^2}{2}a^3 + (5 - p)a + \frac{16w}{9\pi^3} = 0 \qquad (39)$$

The Equation 39 is a cubic equation with respect to a. Roots of a have to be calculated with the given p and w. According to the earlier analysis, for $p > p_k$ and under assumption that $a \geq 0$ there should be two roots, respectively of a_s and a_{ns}, while $a_{ns} < a_s$. To solve the Equation 39 Cardan's formulas will be applied. The Equation 39 can be transformed into

$$a^3 + a(10 - 2p)/(13\pi^2) + (32w)/(117\pi^5) = 0 \qquad (40)$$

The roots of Equation 40 depend on the value of the expression

$$R = (1/4)\left[32w/(117\pi^5)\right]^2 + (1/27)\left[(10 - 2p)/(13\pi^2)\right]^3 \qquad (41)$$

If $p > p_k$, then $R < 0$. It means that the Equation 40 has three real roots.

$$a_{1,2,3} = 2\sqrt{\frac{2p-10}{39\pi^2}}\cos\left(\frac{\lambda}{3} + k\frac{2\pi}{3}\right), \ (k = 0,1,2) \tag{42}$$

The angle λ occurring in the Equation 42 is calculated as follows

$$\cos(\lambda) = -\sqrt{\frac{416w^2}{3\pi^4(p-5)^3}} \tag{43}$$

From the analysis of the function $\cos(\lambda)$ it follows that for $p = p_k$ $\cos(\lambda) = -1$ that is $\lambda = \pi$, while for $p \to \infty$, $\cos(\lambda) \to 0$, so $\lambda \to \pi/2$. The root of a_2 of the Equation 42 for $k = 1$ is always negative, so must be rejected. There are two roots left, of which a_1 (for $k = 0$) is greater than a_3 (for $k = 2$). So we have that

$$a_s = 2\sqrt{\frac{2p-10}{39\pi^2}}\cos\left(\frac{\lambda}{3}\right) \tag{44}$$

$$a_{ns} = 2\sqrt{\frac{2p-10}{39\pi^2}}\cos\left(\frac{\lambda}{3} + \frac{4\pi}{3}\right) \tag{45}$$

where the angle λ is defined by the Equation 43.
For example from Figure 6 we obtain for $w = 3$ and $p = 8$ the values $a_s = 0.1781$, $a_{ns} = 0.0626$.

Discussion of the Range of Values of Axial Force and Continuous Load
In point 2.3 it was stated that a cannot take any optional value due to the specific length of the elastica. Admissible values of a belong to the interval $0 \le a \le a_{gr}$, where $a_{gr} = 3\sqrt{3}/(8\pi) \cong 0.2067$.

On analyzing Figure 5 it is seen that if we increase the value w, then the stable curvilinear solutions a_s located right from the curve g, will be for the value w above a certain amount greater than a_{gr}. Since we try to be always within the admissible limits of the value a, then let us consider what the maximum value w should be for stable curvilinear solutions a_s to belong still to the interval.
Let the value a_k defined by the Equation 38 be less than a_{gr}: $\sqrt[3]{16w/(117\pi^5)} < 3\sqrt{3}/(8\pi)$. Thus

$$w < 9477\sqrt{3}\,\pi^2/8192 = w_{max} \tag{46}$$

Approximately, the boundary value for w amounts to $w_{max} \cong 19.7761$.

Similarly, when looking at Figure 6 it can be seen that with fixed w increasing of the force p above a certain value results in the value a_s greater than the admissible one. Since the value a_s depends not only on the value p, but also on the value λ (dependent in turn on w), thus for various w the maximal values of the axial force p_{max} will be different, and above them there are no more stable curvilinear solutions in the discussed interval of admissible values of a.
In case when $w = 0$ it is sufficient for the value a_m as defined by the Equation 36 was less than a_{gr}. Thus

$$\frac{1}{\pi}\sqrt{\frac{2(p-5)}{13}} < \frac{3\sqrt{3}}{8\pi}$$

and

$$p < 5 + \frac{351}{128} = p_{max}^0 \tag{47}$$

Approximate value of the maximal axial force in case of $w = 0$ amounts to $p_{max}^0 \cong 7,7422$.
For the second case of $w > 0$, the values of p_{max} for subsequent $w \le w_{max}$ were calculated numerically.

To do this, with a fixed w, the value a_s was calculated from the Equation 44 for subsequent forces p increasing by even steps, beginning from the value p_k, till the moment of exceeding the value a_{gr}. Then, the calculation was repeated for the next value of w. From the obtained values, a graph of maximal axial force p_{max} as

function of continuous load w was drawn up. Basing on the Equation 37, also a graph of the critical force p_k as function of continuous load w was made. Both the diagrams are presented in Figure 7.
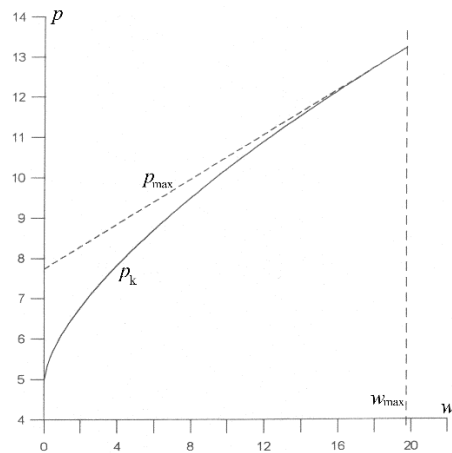
Fig. 7 A graph of the maximal force p_{max} and critical force p_k as function of the continuous load w

IV. Conclusion

In conclusion, let's discuss the problem of stability of the elastica for the case when $w > 0$. As it follows from the above discussion, in this case the rectilinear form of equilibrium will be always stable, while we consider infinitesimal deviations from the point of balance. It can be clearly seen that with the increasing value p the local maximum of energy occurs at a approaching more and more $a = 0$, but not reaching it. It evidences only the fact that for a large value of the force p it is easier to unbalance the system when it is in stable, rectilinear state of equilibrium, causing some finite displacement to it. However, for the system to adopt a new, curvilinear form of stable equilibrium, it is necessary to pass through the maximum of potential energy corresponding to the unstable equilibrium form (Figure 6). The greater the force p, the less displacement must be given to the system in order to reach a new equilibrium form. The force p_k as defined by the Equation 37 can be called the critical force, above which except for the rectilinear form of stability there is also a curvilinear form of stable equilibrium of the system. Due to the assumption of the inextensibility of the elastic, there are the constraints on the value of the shape parameter a, which must be lower than a_{gr}. Hence, further limitations for the value w and the axial force p were occurred, which are illustrated in Figure 7.

The presented stability analysis based on the energy method turned out to be effective. The results can be used for simulation of fabric buckling, folding and for another applications from the field of textile mechanics.

References

[1]. A. G. Greenhill, "Determination Of The Greatest Height Consistent With Stability That A Vertical Pole Or Mast Can Be Made, And Of The Greatest Height To Which A Tree Of Given Proportions Can Grow", Proceedings Of The Cambridge Philosophical Society, Vol. 4, Pp. 65-73, 1881. [Crossref]
[2]. W. G. Bickley, "The Heavy Elastica", Philosophical Magazine, Vol. 17, No. 113, Pp. 603-622, 1934. [Crossref]
[3]. C. Y. Wang, "Large Deformations Of A Heavy Cantilever", Quarterly Of Applied Mathematics, Vol. 39, Pp. 261-273, 1981. [Google Scholar]
[4]. C. Y. Wang, "A Critical Review Of The Heavy Elastica", International Journal Of Mechanical Sciences, Vol. 28, No. 8, Pp. 549-559, 1986. [Crossref]
[5]. S. B. Hsu, S. F. Hwang, "Analysis Of Large Deformation Of A Heavy Cantilever", Siam Journal On Mathematical Analysis, Vol. 19, No. 4, Pp. 854-866, 1988. [Crossref] [Google Scholar]
[6]. T. Beléndez, M. Pérez-Polo, C. Neipp, A. Beléndez, "Numerical And Experimental Analysis Of Large Deflections Of Cantilever Beams Under A Combined Load", Physica Scripta, Vol. 2005, No. T118, Pp. 61-65, 2005. [Crossref]
[7]. P. B. Gonçalves, D. Jurjo, C. Magluta, N. Roitman, D. Pamplona, "Large Deflection Behavior And Stability Of Slender Bars Under Self Weight", Structural Engineering And Mechanics, Vol. 24, Pp. 709-725, 2006. [Crossref]
[8]. S. T. Santillan, R. H. Plaut, T. P. Witelski, L. N. Virgin "Large Oscillations Of Beams And Columns Including Self-Weight", International Journal Of Non-Linear Mechanics, Vol. 43, No. 8, Pp. 761-771, 2008. [Crossref]
[9]. A. N. Dinnik, Buckling And Torsion, Academy Of Sciences Of The Soviet Union, Moscow, Russia, 1955 (In Russian). [Google Scholar]
[10]. X. Zhang, J. Yang, "Inverse Problem Of Elastica Of A Variable-Arc-Length Beam Subjected To A Concentrated Load", Acta Mechanica Sinica, Vol. 21, No. 5, Pp. 444-450, 2005. [Google Scholar] [Publisher Link]
[11]. J. S. Chen, H. C. Li, W. C. Ro, "Slip-Through Of A Heavy Elastica On Point Supports", International Journal Of Solids And Structures, Vol. 47, No. 2, Pp. 261-268, 2010. [Google Scholar] [Publisher Link]
[12]. F. C. Onyeka, E. T. Okeke, "Analytical Solution Of Thick Rectangular Plate With Clamped And Free Support Boundary Condition Using Polynomial Shear Deformation Theory" Advances In Science, Technology And Engineering Systems Journal, Vol. 6, No. 1, Pp. 1427-1439, 2021. [Crossref]
[13]. A. Hassan, N. Kurgan, "Modeling And Buckling Analysis Of Rectangular Plates In Ansys" International Journal Of Engineering And

Applied Sciences, Vol. 11, No. 1, Pp. 310-329, 2019. [Crossref]

[14]. F. C. Onyeka, B. O. Mama, C. D. Nwa-David, "Analytical Modelling Of A Three-Dimensional (3d) Rectangular Plate Using The Exact Solution Approach" Iosr Journal Of Mechanical And Civil Engineering, Vol. 19, No. 1, Ser. 1, Pp. 76-88, 2022. [Publisher Link]

[15]. F. C. Onyeka, F. O. Okafor, H. N. Onah, "Buckling Solution Of A Three-Dimensional Clamped Rectangular Thick Plate Using Direct Variational Method", Iosr Journal Of Mechanical And Civil Engineering, Vol. 18, No. 3, Ser. 3, Pp. 10-22, 2021. [Publisher Link]

[16]. F. C. Onyeka, D. Osegbowa, E. E. Arinze, "Application Of A New Refined Shear Deformation Theory For The Analysis Of Thick Rectangular Plates", Nigerian Research Journal Of Engineering And Environmental Sciences, Vol. 5, No. 2, Pp. 901-917, 2020. [Publisher Link]

[17]. C. C. Ike, "Kantorovich-Euler Lagrange-Galerkin's Method For Bending Analysis Of Thin Plates", Nigerian Journal Of Technology, Vol. 36, No. 2, Pp. 351-360, 2017. [Publisher Link]

[18]. J. N. Reddy, Classical Theory Of Plates, In Theory And Analysis Of Elastic Plates And Shells, 2nd Ed., Crc Press, Boca Raton, Fl, Usa, 2006. [Crossref]

[19]. R. D. Mindlin, "Influence Of Rotatory Inertia And Shear On Flexural Motions Of Isotropic, Elastic Plates", Journal Of Applied Mechanics, Transactions Asme, Vol. 18, No. 1, Pp. 31-38, 1951. [Crossref]

[20]. F. C. Onyeka, O. M. Ibearugbulem, "Load Analysis And Bending Solutions Of Rectangular Thick Plate", International Journal On Emerging Technologies, Vol. 11, No. 3, Pp. 1103-1110, 2020. [Google Scholar]

[21]. F. C. Onyeka, E. T. Okeke, J. Wasiu, "Strain-Displacement Expressions And Their Effect On The Deflection And Strength Of Plate", Advances In Science, Technology And Engineering Systems, Vol. 5, No. 5, Pp. 401-413, 2020. [Crossref]

[22]. A. S. Sayyad, Y. M. Ghugal, "Bending And Free Vibration Analysis Of Thick Isotropic Plates By Using Exponential Shear Deformation Theory", Journal Of Applied And Computational Mechanics, Vol. 6, Pp. 65-82, 2012. [Google Scholar]

[23]. F. C. Onyeka, B. O. Mama, C. D. Nwa-David. "Application Of Variation Method In Three Dimensional Stability Analysis Of Rectangular Plate Using Various Exact Shape Functions", Nigerian Journal Of Technology, Vol. 41, No. 1, Pp. 8-20, 2022. [Crossref]

[24]. S. M. Gunjal, R. B. Hajare, A. S. Sayyad, M. D. Ghodle, "Buckling Analysis Of Thick Plates Using Refined Trigonometric Shear Deformation Theory", Journal Of Materials And Engineering Structures, Vol. 2, No. 4, Pp. 159-167, 2015. [Google Scholar]

[25]. J. C. Ezeh, I. C. Onyechere, O. M. Ibearugbulem, U. C. Anya, L. Anyaogu, "Buckling Analysis Of Thick Rectangular Flat Ssss Plates Using Polynomial Displacement Functions", International Journal Of Scientific & Engineering Research, Vol. 9, No. 9, Pp. 387-392, 2018. [Google Scholar]

[26]. F. C. Onyeka, B.O. Mama, T. E. Okeke, "Exact Three-Dimensional Stability Analysis Of Plate Using A Direct Variational Energy Method", Civil Engineering Journal, Vol. 8, No. 1, Pp. 60-80, 2022. [Crossref].

[27]. V. T. Ibeabuchi, O. M. Ibearugbulem, C. Ezeah, O. O. Ugwu, "Elastic Buckling Analysis Of Uniaxially Compressed Cccc Stiffened Isotropic Plates", International Journal Of Applied Mechanics And Engineering, Vol. 25, No. 4, Pp. 84-95, 2020. [Crossref]

[28]. F. C. Onyeka, F. O. Okafor, H. N. Onah, "Buckling Solution Of A Three-Dimensional Clamped Rectangular Thick Plate Using Direct Variational Method", Iosr Journal Of Mechanical And Civil Engineering, Vol. 18, No. 3, Ser. 3, Pp. 10-22, 2021. [Publisher Link]

[29]. F. C. Onyeka, F. O. Okafor, H. N. Onah, "Application Of A New Trigonometric Theory In The Buckling Analysis Of Three-Dimensional Thick Plate", International Journal Of Emerging Technologies, Vol. 12, No. 1, Pp. 228-240, 2021. [Publisher Link]

[30]. C. L. Dym, Stability Theory And Its Applications To Structural Mechanics, Noordhoff International Publishing Company: Leyden, Netherlands, Pp. 1-47, 1974. [Crossref]